Mammalian diaphanous-related formin Dia1 controls the organization of E-cadherin-mediated cell-cell junctions

Letizia Carramusa[1], Christoph Ballestrem[2], Yuliya Zilberman[1] and Alexander D. Bershadsky[1,*]

[1]Department of Molecular Cell Biology, The Weizmann Institute of Science, PO Box 26, Rehovot 76100, Israel
[2]The Wellcome Trust Centre for Cell-Matrix Research, University of Manchester, Faculty of Life Sciences, Oxford Road, Manchester M13 9PT, UK
*Author for correspondence (e-mail: alexander.bershadsky@weizmann.ac.il)

Accepted 13 August 2007
Journal of Cell Science 120, 3870-3882 Published by The Company of Biologists 2007
doi:10.1242/jcs.014365

Summary

The formin-homology protein Dia1 is a target of RhoA and a potent activator of nucleation and elongation of actin filaments. Here, we demonstrate that short-hairpin (sh) RNA-mediated downregulation of Dia1 in human MCF7 epithelial cells disrupts adherens junctions, as manifested by the significantly decreased localization of E-cadherin and associated proteins to cell-cell contacts. Expression of mouse Dia1, which is insensitive to the human Dia1-specific shRNA, rescued the junctional integrity. Coexpression of GFP-tagged Dia1 and a constitutively active RhoA mutant, RhoA-V14, resulted in localization of the exogenous GFP-Dia1 to the cell-cell junctions. This localization was accompanied by a strong increase in the width of the adhesion zone and augmentation of the actin, E-cadherin and β-catenin content of the junctions. A constitutively active Dia1 mutant lacking the N-terminal portion was unable to localize to cell-cell junctions and did not show any junction-strengthening effect. The adherens junction enhancement induced by Dia1 and active RhoA did not require microtubules, but depended on the activity of myosin II. Inhibition of myosin II activity abolished the Dia1-mediated reinforcement of cell-cell junctions and instead induced the formation of numerous actin-rich filopodia at the contact zone. Thus, Dia1 localizes to and controls cadherin-mediated junctions in a RhoA-dependent manner.

Supplementary material available online at
http://jcs.biologists.org/cgi/content/full/120/21/3870/DC1

Key words: Actin polymerization, Adherens junctions, RNAi, RhoA, Formins, Myosin II

Introduction

It is well established that both the formation and maintenance of cell-cell junctions in epithelial cells depend on the actin cytoskeleton. Formation of cadherin-mediated cell-cell junctions (adherens junctions) is accompanied by profound changes in the actin cytoskeleton and accumulation of polymerized actin at the contact area (Bershadsky, 2004; Mege et al., 2006). Inhibition of actin assembly by treatment with pharmacological reagents such as latrunculin or cytochalasin prevents the formation and strengthening of cadherin-mediated adhesions in addition to disrupting those already in existence (Angres et al., 1996; Chu et al., 2004; Ivanov et al., 2005; Vasioukhin et al., 2000). However, the molecular mechanisms underlying the crosstalk between cadherin signaling and the actin cytoskeleton are not fully understood. In particular, the specific role of proteins regulating actin polymerization in the formation and maintenance of the adhesion contacts has yet to be elucidated.

The basic unit of the adherens junction is a cadherin-catenin complex, which consists of transmembrane adhesion receptors known as classic cadherins. These interact in a homophilic manner with the cadherins of neighboring cells. The cytoplasmic domains of classic cadherins interact directly with proteins of the armadillo family: p120 catenin by means of the juxtamembrane domain, and β-catenin or plakoglobin by means of the C-terminal domain. Both β-catenin and plakoglobin can bind to α-catenin, which is another essential element of the cadherin-catenin complex (for reviews, see Gumbiner, 2005; Perez-Moreno and Fuchs, 2006; Wheelock and Johnson, 2003). Monomeric α-catenin interacts with β-catenin or plakoglobin, whereas homodimers of α-catenin can bind to actin filaments and regulate their polymerization and crosslinking (Weis and Nelson, 2006). p120 catenin is another protein functioning at the interface between cadherin and actin, and this regulates Rho GTPases (Reynolds, 2007) and interacts with the actin-binding protein cortactin (Boguslavsky et al., 2007).

Regulators of actin nucleation appear to be crucial for the control of cadherin-mediated cell-cell adhesion. For example, the Arp2/3 complex, which promotes the formation of a branched actin filament network (Higgs and Pollard, 2001; Nicholson-Dykstra et al., 2005), localizes to adherens junctions and physically associates with the cadherin-catenin complex (Kovacs et al., 2002; Verma et al., 2004). Moreover, activators of Arp2/3 function, WAVE (Yamazaki et al., 2006), N-WASP (Ivanov et al., 2005) and cortactin (El Sayegh et al., 2004; Helwani et al., 2004), demonstrate a similar localization. Knockdowns of these components induce weakening of adherens junctions, exemplified by the reduced density of cadherin and its associated proteins.

Another group of molecules controlling actin polymerization comprises proteins of the formin family, which

are characterized by the presence of highly conserved formin-homology 1 and 2 (FH1 and FH2) domains and are involved in nucleating the polymerization of linear actin filaments and promoting their elongation (Faix and Grosse, 2006; Goode and Eck, 2007; Higgs, 2005). Formin-1, which was historically the first representative of this group of proteins, is now known to be a partner for α-catenin (Kobielak et al., 2004). Formin-1 localizes to cadherin-mediated cell-cell junctions in an α-catenin-dependent manner; its association with the cadherin-catenin complex is necessary for the formation and maintenance of adherens junctions in keratinocytes (Kobielak et al., 2004).

The potential role in cadherin-mediated adhesion of Diaphanous-related formins is of particular interest as their activity is controlled by small G-proteins of the Rho family (Faix and Grosse, 2006; Higgs, 2005; Olson, 2003). In several cell types, Rho, Rac and Cdc42 are essential for, and activated by, cadherin-mediated cell-cell adhesion (Braga, 2002). Although the roles of Cdc42 and, especially, Rac can at least partially be related to the regulation of Arp2/3-mediated actin polymerization (Kraemer et al., 2007; Yamazaki et al., 2006), the mechanism underlying the apparent Rho dependence of adherens junctions (Braga et al., 1997; Sahai and Marshall, 2002) is still poorly understood. Diaphanous-related formin 1 (Dia1) is one of the Rho targets; RhoA binding triggers the transition of Dia1 from a closed, inactive conformation to an open, active conformation (Li and Higgs, 2003; Otomo et al., 2005; Rose et al., 2005). It has been reported that the disruption of adherens junctions induced by inhibition of Rho could be rescued by overexpression of a constitutively active form of Dia1 (Sahai and Marshall, 2002). This finding suggests that Dia1 participates in the Rho-dependent regulation of adherens junctions.

Here, an RNAi-mediated silencing approach was used to demonstrate that Dia1 is required for the integrity of adherens junctions. Moreover, we show that, upon activation by RhoA, Dia1 localizes to adherens junctions, which leads to their dramatic strengthening and enlargement. Our data therefore show that the formin protein Dia1 is an indispensable component and a potent regulator of cell-cell junctions in epithelial cells.

Results

Knockdown of Dia1 suppresses the junctional localization of E-cadherin

To investigate the role of Dia1 in cell-cell adhesions, we selected the MCF7 human breast cancer epithelial cell line. These cells preserve normal epithelial E-cadherin-mediated adherens junctions enriched in α- and β-catenins, actin and actin-associated proteins, including vasodilator-stimulated phosphoprotein (VASP), as well as apical tight junctions (van Deurs et al., 1987). Immunofluorescence staining with an antibody against Dia1 revealed a diffuse distribution of the endogenous protein over the cytoplasm, with some weak enrichment at the cell-cell contacts (Fig. 1A-C).

To analyze the role of Dia1 in the formation of cell-cell junctions, we transiently transfected cells with a pSuper vector (Brummelkamp et al., 2002) bearing short hairpin RNA sequences (shRNA) specific for the silencing of expression of human Dia1 (hDia1; si-hDia1 vector). To mark the transfected cells, we co-transfected the shRNA-encoding plasmid with the pGFP-C1 plasmid. Control cells were transfected with pGFP-C1 together with an empty pSuper vector. Expression of si-hDia1 led to a significant decrease of hDia1 in MCF7 cells, as revealed by western blot analysis of GFP-labelled cells (Fig. 1D) and immunofluorescence staining with an antibody against Dia1 (Fig. 1E,F). Densitometric measurement of the levels of Dia1 showed that less than 10% of the endogenous Dia1 remained in the cells expressing si-hDia1.

Comparison of E-cadherin staining in control and hDia1-knockdown MCF7 cells showed a dramatic decrease in E-cadherin localization at the shared cell borders, especially when both neighboring cells were depleted of Dia1 (compare Fig. 1H with K). In >80% of such cell pairs, the cell-cell junctions marked by E-cadherin staining were abnormal, that is either were not distinguishable at all or were discontinuous and less intensely stained than junctions in control cells (Fig. 1K,M). Intercellular contacts between Dia1-deficient and neighboring control cells preserved normal E-cadherin-staining in less than 60% of the cases (Fig. 1M). Among control cells (both non-transfected, or transfected with empty pSuper plasmid), more than 80% of junctions preserved a normal (uniformly bright) E-cadherin staining pattern (Fig. 1H,M). Differences in actin staining along contacting cell borders were, however, less pronounced (Fig. 1I,L).

The localization of E-cadherin at the junctions of hDia1-knockdown cells can be restored by ectopic expression of mouse Dia1.

To confirm that the phenotype observed in si-hDia1 cells is due to the suppression of the target protein, we performed rescue experiments (Fig. 2A-G). For such experiments, we co-transfected human MCF7 cells with the si-hDia1 vector and with a vector encoding GFP-fused mouse Dia1 (mDia1), the sequence of which contained three nucleotide mismatches compared with the human Dia1-shRNA sequence (Fig. 2A). The human shRNA sequence that knocked-down Dia1 in human cells did not affect expression of GFP-mDia1. Indeed, western blot analysis of the cell lysates with the non-species-specific antibody against Dia1 revealed that, although the amount of endogenous hDia1 decreased in the cells expressing si-hDia1, the amount of GFP-mDia1 did not change (Fig. 2B). Although transfection with the si-hDia1 vector alone abolished E-cadherin localization to cell-cell junctions, as in our previous experiments (Fig. 2C,D), the cells transfected with si-hDia1 and therefore lacking endogenous Dia1, but expressing GFP-mDia1, showed prominent localization of E-cadherin to cell-cell junctions (Fig. 2E,F). Scoring of the intact E-cadherin-positive contacts (Fig. 2G) confirmed that expression of GFP-mDia1 is sufficient to restore the junctional localization of E-cadherin in the cells transfected with the si-hDia1 vector, showing that loss of E-cadherin localization was indeed the result of downregulation of hDia1.

Analysis of the junction-associated protein distribution in the Dia1-knockdown cells

To assess quantitatively the changes in the junctional proteins upon Dia1 knockdown, we first compared total E-cadherin and β-catenin amounts in control and knockdown cells by western blotting. In these experiments, MCF7 cells stably transfected with the pSuper-retro-shLacZ (control) and the pSuper-retro-shDia1 vectors were analyzed (Fig. 3A,B). Densitometric

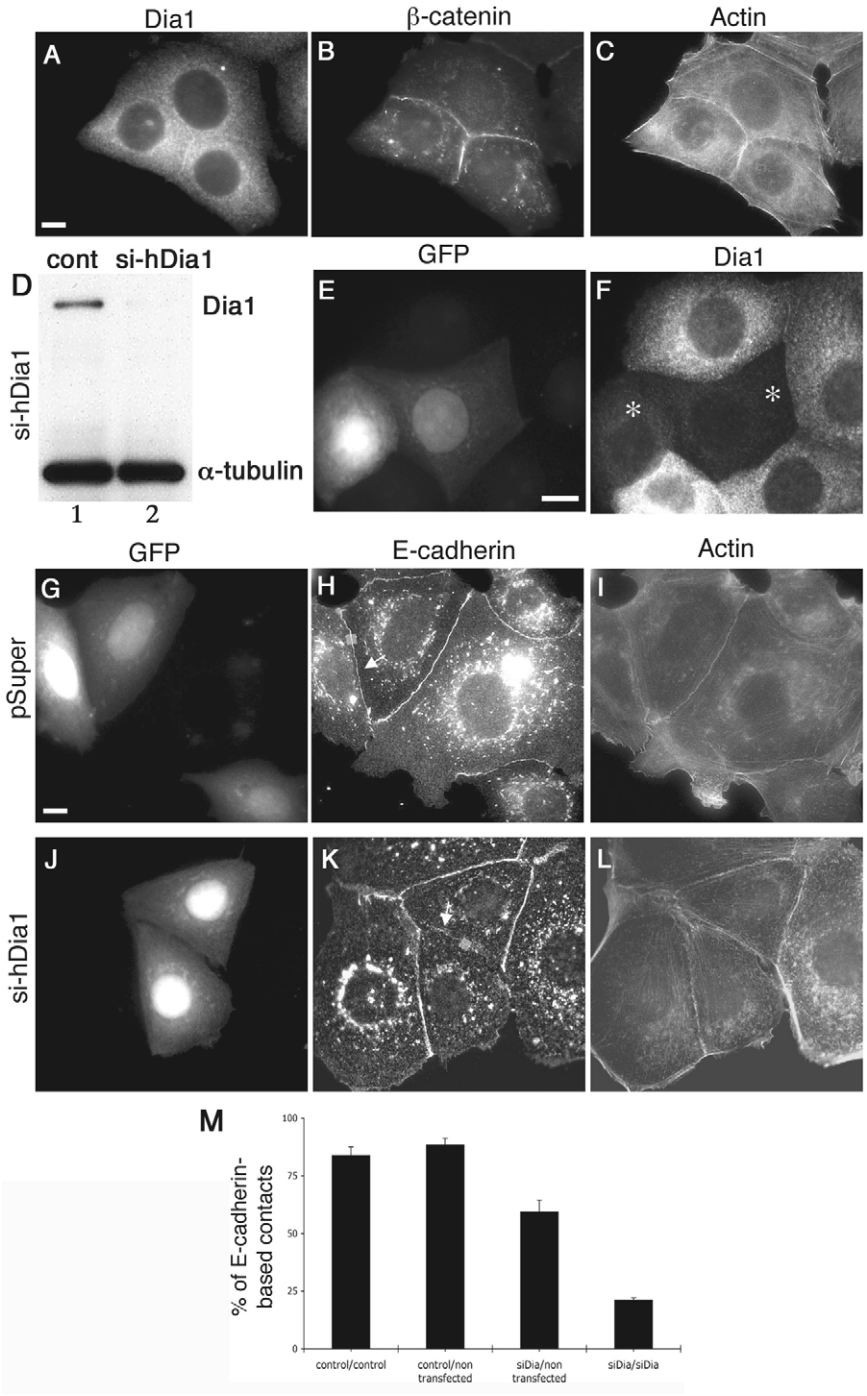

Fig. 1. Effect of Dia1 knockdown on the integrity of adherens junctions in MCF7 cells. (A) Distribution of endogenous hDia1 in MCF7 cells, as revealed by antibody staining. Note some enrichment at cell-cell contacts. (B) β-catenin and (C) actin stainings of the same field. (D) Western blot of MCF7 cells transfected with a GFP expression vector and either pSuper vector (cont; lane 1) or a shRNA sequence for human Dia1 cloned in a pSuper vector (si-hDia1; lane 2). GFP-expressing cells were collected by FACS sorting 72 hours after transfection. The blot was probed with antibody against Dia1, and an antibody against tubulin as a loading control. (E,F) Depletion of Dia1 by interfering RNA. MCF7 cells co-transfected with pGFP-C1 and pSuper si-hDia1 were stained with antibody against Dia1 72 hours following transfection. Dia1 is reduced dramatically in cells coexpressing the GFP marker (F, asterisks). (G-L) E-cadherin localization in control and si-hDia1-expressing cells. E-cadherin staining in control cells (H) and hDia1-knockdown cells (K) shows that the localization of E-cadherin at cell-cell borders is dramatically reduced in Dia1-knockdown cells (arrows). GFP labeling of transfected cells is shown in (G,J) and actin staining is shown in (I,L). White boxes in the images H and K are used for quantification (see Fig. 3C,D). Bars, 10 μm. (M) Assessment of intact E-cadherin-containing cell-cell contacts in control and hDia1-knockdown cells. The mean percentage of intact E-cadherin-positive contacts is shown by bars. Quantification was done for three independent experiments, including measurements of 30 pairs of cells for each experiment. Error bars represent standard deviations (s.d.).

analysis of the western blots revealed that, in spite of a >90% reduction in the hDia1 expression, the amounts of E-cadherin and β-catenin (normalized against the levels of α-tubulin in the corresponding samples) did not decrease (Fig. 3B).

To quantify the levels of E-cadherin and actin localized to cell-cell junctions, we scanned the fluorescence intensity along segments crossing the junctions in a perpendicular direction (small squares in Fig. 1H,K). In control cells, such scanning revealed narrow maxima of fluorescence ('peaks') corresponding to the junctions (Fig. 3C). For the analysis of the junctions in Dia1-knockdown cells, we chose only those fluorescence profiles on which the fluorescence peaks were distinguishable (Fig, 3D). Comparison of the fluorescence intensities corresponding to the peak values revealed that, even in these partially preserved junctions between Dia1-knockdown cells, the fluorescence intensity of E-cadherin was reduced on average by ~50% in comparison with that of the control (Fig. 3E, black bars). At the same time, there were no significant differences between the average levels of cytoplasmic E-cadherin fluorescence between control and Dia1-knockdown cells (data not shown). A similar analysis, measuring the phalloidin fluorescence corresponding to peak values at the cell-cell interface, revealed a slight, albeit statistically significant, decrease of the junctional actin in Dia1-knockdown cells (Fig. 3E, gray bars). It should be noted that these measurements quantify junctional actin (Zhang et al., 2005), but not the actin of peripheral bundles sometimes found adjacent to the junctions.

To investigate how Dia1 knockdown affects the localization of other major components of adherens junctions, we performed immunofluorescence experiments with antibodies against α-catenin (Figs 4 and 5) and β-catenin (Fig. 4). We also

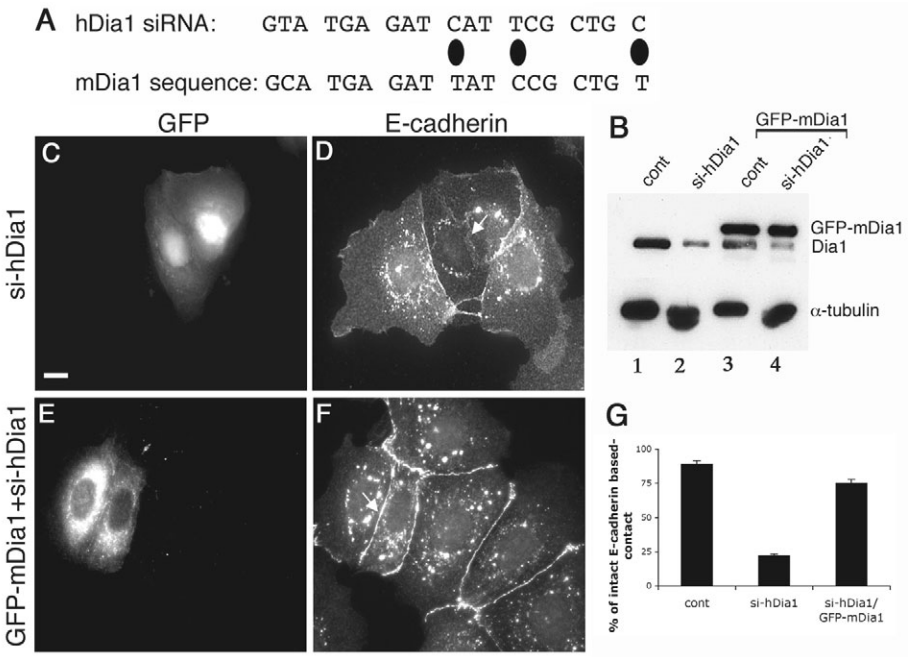

Fig. 2. Ectopic expression of mouse Dia1 rescues the effect of human Dia1 knockdown on cell-cell junctions. (A) The human Dia1-siRNA sequence used to knockdown the endogenous Dia1 contains three nucleotide mismatches compared with the sequence of mouse Dia1 (mDia1; black ovals). (B) The expression of GFP-mDia1 full-length protein is not affected by the hDia1-siRNA sequence. Control MCF7 cells, stably expressing the shRNA against LacZ (cont; lane 1) and cells stably expressing the shRNA against hDia1 (lane 2) were transiently transfected with the GFP-mDia1 plasmid (lanes 3, 4). Western blots of whole-cell lysates show that exogenous mDia1 is expressed at the correct molecular mass in the hDia1-knockdown cells (lane 4). (C,D) Expression of pSuper si-hDia1 leads to disappearance of E-cadherin staining from the interface between transfected (GFP-labeled) cells. (E,F) In cells expressing the GFP-mDia1 protein together with the human Dia1-siRNA plasmid, E-cadherin staining is as prominent as in the neighboring control cells. Bar, 10 μm. (G) Assessment of E-cadherin-containing cell-cell contacts in control cells, in hDia1-knockdown cells and in cells expressing the GFP-mDia1 protein together with the human Dia1-siRNA plasmid. Bars show the mean percentage of intact E-cadherin-positive contacts between transfected cells; error bars represent standard deviations (s.d.).

assessed the localization of the actin-binding protein VASP, known to be an important modulator of actin organization at adherens junctions (Scott et al., 2006; Vasioukhin et al., 2000) (Fig. 5). As intercellular junctions are sites of high protein tyrosine kinase and phosphatase activity (Sallee et al., 2006; Volberg et al., 1991), we also probed the distribution of tyrosine-phosphorylated junctional components using an antibody detecting phosphotyrosine (Fig. 5). The stainings revealed that, as with E-cadherin localization, the localizations of all the aforementioned components were strongly diminished at the cell-cell interface of Dia1-knockdown cells in comparison with the junctions between control and knockout cells or between two control cells.

MCF7 cells can form tight junctions (van Deurs et al., 1987) and, as shown in supplementary material Fig. S1A-C, express and localize to the cell-cell junctions the protein cingulin, a bona fide component of tight junctions (Citi et al., 1988). Downregulation of mDia1 led to disappearance of the junctional cingulin staining from some, but not all, junctions between affected cells. In particular, some junctions lacking E-cadherin demonstrated well-preserved cingulin localization (supplementary material Fig. S1D-F). In some cases, however, the junctions between Dia1-knockdown cells demonstrated staining for neither E-cadherin nor cingulin (supplementary material Fig. S2A).

To reveal differences in the de novo formation of junctions between control and Dia1-deficient cells, the junctions were disrupted by Ca^{2+} depletion and then allowed to recover at the normal Ca^{2+} concentration (supplementary material Fig. S2). Non-transfected cells, or cells transfected with GFP and empty pSuper vector, restored the junctions almost completely in 30-60 minutes following the Ca^{2+} switch, as revealed by stainings for E-cadherin, actin and cingulin (supplementary material Fig. S2A,B). Dia1-knockdown cells were apparently more sensitive to Ca^{2+} depletion than control cells (supplementary material Fig. S2A). After the Ca^{2+} switch, these cells restored their spread morphology and showed F-actin accumulation at the cell-cell interfaces. Nevertheless, only a small fraction of the junctions between GFP-labelled si-hDia1-expressing cells demonstrated proper E-cadherin or cingulin localization even 2 hours after the Ca^{2+} switch (supplementary material Fig. S2A,C). Thus, Dia1 is required for the formation of junctional complexes typical of normal epithelial cells.

Dia1 localizes to adherens junctions in a Rho-dependent manner and strengthens adherens junctions

As Dia1 is required for the integrity of the adherens junctions, we investigated whether it localized to these structures. As mentioned above, staining of MCF7 cells with an antibody specific for Dia1 showed a diffuse distribution in the cytoplasm, with some weak enrichment at regions of cell-cell junctions (Fig. 1A-C). Transfection of MCF7 cells with a construct encoding full-length mouse Dia1 protein (GFP-mDia1) showed that full-length mDia1 was diffusely distributed in the whole cytoplasm and did not demonstrate any apparent enrichment at the cell-cell junctions (Fig. 6A). Neither the actin cytoskeleton nor the adherens junctions of the cells were affected by the overexpression of full-length mDia1, as revealed by staining for actin and β-catenin (Fig. 6B,C). However, when full-length mDia1 was coexpressed with a constitutively active RhoA protein (RhoA-V14), a significant enrichment of mDia1 was observed at the junctions between affected cells (Fig. 6D). As active RhoA triggers a transition of Dia1 from an inactive 'closed' to an active 'open' conformation (Li and Higgs, 2003; Otomo et al., 2005; Rose et al., 2005), this result demonstrates that the activation of the

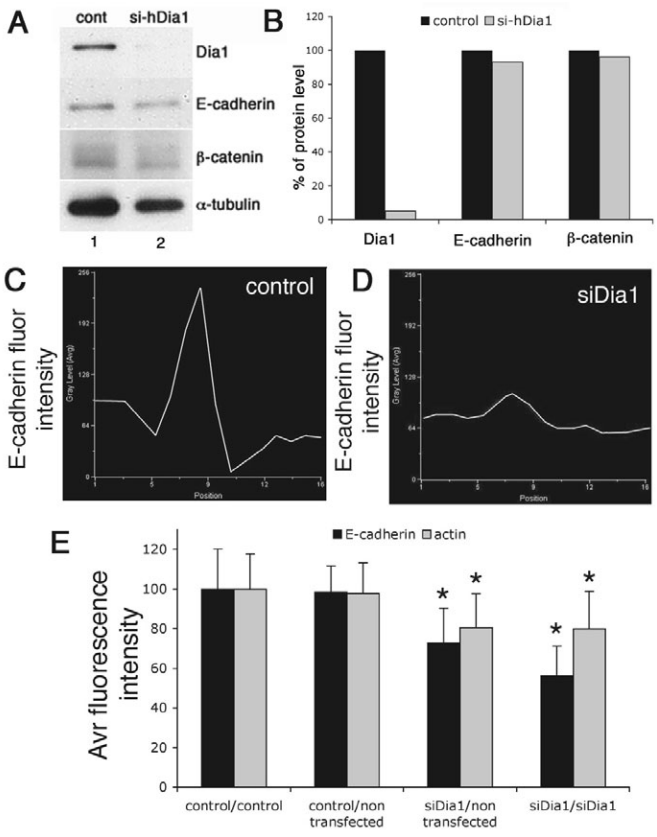

Fig. 3. Assessment of junction-associated protein distribution. (A-B) E-cadherin and β-catenin levels are not reduced in the Dia1-knockdown cells. (A) Western blot of cell lysates from cells stably expressing the shRNA against LacZ (cont; lane 1) and cells stably expressing the shRNA against hDia1 (lane 2) blotted for E-cadherin and β-catenin. Blotting for α-tubulin was used as a loading control. (B) Quantitative measurement of Dia1, E-cadherin and β-catenin levels, adjusted for the difference in gel loading. Values for control cells were taken as 100%. (C,D) The fluorescence intensity of E-cadherin and actin at cell-cell contacts is reduced in the Dia1-knockdown cells. Representative plot profiles of E-cadherin fluorescence intensity at cell-cell contacts in control (C) and knockdown (D) cells. The white boxes in Fig. 1H,K mark the regions corresponding to plots C and D, respectively. (E) Quantification of the fluorescence intensity of E-cadherin and actin at cell-cell contacts measured by line-scan analysis on digital images. Bars represent the average fluorescence intensity expressed in arbitrary units. Error bars represent s.d. values. Asterisks indicate the values that differ significantly from corresponding controls (Student's *t*-test, $P<0.0001$).

mDia1 molecule strongly enhances its affinity for the junctions.

To assess quantitatively the effect of RhoA-mediated activation on localization of GFP-mDia1, we measured the GFP fluorescence profiles along segments crossing the cell-cell interfaces visualized by E-cadherin or β-catenin immunofluorescence. We calculated a GFP-mDia1 localization index as the difference between fluorescence intensities at the cell-cell interface and in the adjacent cytoplasm, normalized to the fluorescence intensity value obtained for the cytoplasm (Fig. 6J). The difference between the distributions of GFP-mDia1 in control and RhoA-V14-expressing cells was dramatic. The junctional fluorescence in cells transfected with GFP-mDia1 alone was lower than the fluorescence in the cytoplasm, whereas, in the presence of active Rho, the fluorescence intensity of GFP-mDia1 at the junctions was significantly higher than in the cytoplasm (Fig. 6J). Interestingly, this effect was observed when both of the cells in contact were affected. At the interface between cells expressing GFP-mDia1 plus RhoA-V14 and control, non-transfected cells, the former produced numerous filopodial projections with GFP-mDia1 localized to their tips (Fig. 6D inset), but enrichment of junctional GFP-mDia1 was not observed.

As could be predicted from previous studies (Tominaga et al., 2000; Watanabe et al., 1999; Watanabe et al., 1997), the coexpression of GFP-mDia1 and RhoA-V14 triggered the formation of numerous bundles of actin filaments (Fig. 6E). Furthermore, the level of junctional F-actin increased at the contacts between such cells, in comparison with that of non-transfected cells or cells expressing only GFP-mDia1 [Fig. 6E (arrow) and 6K, gray bars]. Remarkably, coexpression of GFP-mDia1 and RhoA-V14 not only increased the junctional levels of GFP-mDia1 and F-actin but also strongly promoted accumulation of β-catenin at the cell-cell junctions (Fig. 6F). This result again was most apparent when both neighboring cells expressed GFP-mDia1 and RhoA-V14. β-Catenin staining at the interface between such cells was much stronger than at the contacts between cells expressing GFP-mDia1 only, or between two non-transfected cells [Fig. 6F (arrow) and 6K, black bars]. The junctional levels of E-cadherin (Fig. 7A,B) and α-catenin (not shown) were also dramatically augmented. Examination of the cells expressing GFP-mDia1 plus RhoA-V14 by confocal microscopy (Fig. 7A-E) revealed that the average height of the E-cadherin-positive junctions between such cells at the *X-Z* plane [Fig. 7C,D (arrows)] increased approximately twofold in comparison with the height of junctions between control cells (Fig. 7C-E). Thus, coexpression of exogenous mDia1 and constitutively active RhoA increases the width of the 'adhesion belt' between the affected cells.

Not only exogenous GFP-mDia1 but also endogenous Dia1 translocates to the junctions upon expression of constitutively active RhoA-V14. In the RhoA-V14-transfected culture, cells expressing active Rho formed prominent actin bundles and demonstrated spectacular localization of endogenous hDia1 to the contact between affected cells (Fig. 6G,H). This was accompanied by some enhancement of cell-cell junctions, as revealed by staining for β-catenin (Fig. 6I and supplementary material Fig. S3C). The effect on β-catenin recruitment was, however, less prominent in cells transfected with RhoA-V14 alone than in the cells coexpressing RhoA-V14 with GFP-mDia1 (compare Fig. 6F with 6I and supplementary material Fig. S3C).

It is worth noting that expression of RhoA-V14 did not result in any enhancement of cell-cell junctions in the cells with downregulated endogenous hDia1 (supplementary material Fig. S3D-F). Assessment of the β-catenin-positive contacts between cells coexpressing GFP-RhoA-V14 and si-hDia1 revealed that the percentage of normal junctions between these cells was as low as that between cells expressing si-hDia1 only (supplementary material Fig. S3G). These results, therefore,

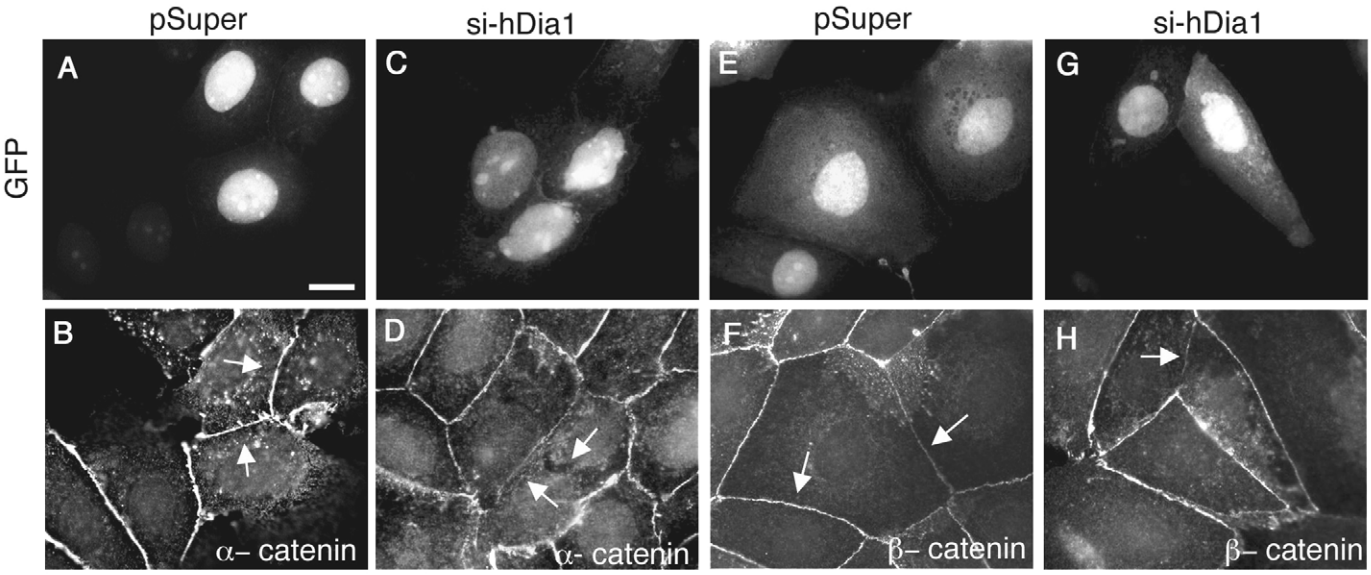

Fig. 4. Effect of Dia1 knockdown on the distribution of α- and β-catenin. Immunofluorescence of cells transfected with a GFP-encoding vector together with either an empty pSuper vector (A,B and E,F) or pSuper si-hDia1 (C,D and G,H) stained with antibodies against α-catenin (B,D) and β-catenin (F,H). Arrows indicate cell-cell junctions. Note that both α- and β-catenins are enriched and uniformly distributed along the cell-cell junctions in control cells (B,F), whereas junctions between Dia1-knockdown cells show reduced and fragmented staining (D,H). Bar, 10 μm.

show that Dia1 is a Rho target that is required for the stimulatory effect of Rho on the cell-cell adherens junctions.

Molecular requirements for the Dia1 junctional localization

Dia1 activation by itself was not sufficient for the localization of this protein to adherens junctions as truncated constitutively active forms of mDia1 (Fig. 8A) (Watanabe et al., 1999), mDia1-ΔN1, mDia1-ΔN2 and mDia1-ΔN3 did not localize to adherens junctions (Fig. 8B; and data not shown) and did not increase the levels of junctional actin and β-catenin (Fig. 8C,D). To analyze further the molecular requirements for the junctional localization of Dia1, we prepared mDia1 that lacked the C-terminal DAD domain but had an intact N-terminal region (Fig. 8A). Owing to the absence of the DAD domain, this mutant (CFP-mDia1-ΔDAD) maintains its open conformation with a freely accessible Rho-binding domain (Otomo et al., 2005; Rose et al., 2005). Its overexpression should therefore lead to Rho sequestration and produce a phenotype resembling that induced by inhibition of endogenous Rho. Indeed, when the level of CFP-mDia1-ΔDAD expression was high, the transfected cells had an altered morphology and the integrity of the cell-cell junctions was often disrupted in the same way as in cells transfected with dominant-negative Rho (data not shown). However, at moderate expression levels, when intact adherens junctions were still preserved, CFP-mDia1-ΔDAD clearly localized to cell-cell junctions (Fig. 8E).

Thus, the N-terminal region of mDia1 (residues 1-263) seems to be involved in the localization of Dia1 to the junctions. Surprisingly, coexpression of mDia1-ΔN3 together with constitutively active RhoA was sufficient to produce some mDia1-ΔN3 localization to the cell-cell junctions (Fig. 8F); however this was less prominent than the localization of CFP-mDia1-ΔDAD under the same conditions (Fig. 8G).

Taken together, these results suggest that not only activation but also the junctional localization of Dia1 is required for the augmentation of adherens junctions. Our data are consistent with the idea that the N-terminal region of Dia1 is important for the correct localization of the activated Dia1 to cell-cell junctions. In addition, we found evidence for an additional, N-terminus-independent, mechanism of Dia1 junctional localization that apparently depends on RhoA.

The role of microtubules and myosin II activity in the Dia1 function at adherens junctions

In view of the accumulating data on the involvement of microtubules in the regulation of cell-cell junctions (Ivanov et al., 2006; Mary et al., 2002; Stehbens et al., 2006; Waterman-Storer et al., 2000), we tested whether microtubules are important for the effect of Dia1 on adherens junctions. We added nocodazole to the cells co-transfected with RhoA-V14 and GFP-mDia1 four hours after transfection, so that expression of these proteins occurred in conditions of microtubule disruption. In control cells, with intact microtubules, expression of GFP-mDia1 and RhoA-V14 led to the localization of GFP-mDia1 to the cell-cell junctions and a significant enhancement of adhesion protein recruitment to these structures (Fig. 6D-F and Fig. 9A-C). Incubation with nocodazole was sufficient to disrupt the microtubule network of affected cells almost completely (compare Fig. 9A with D). In cells lacking microtubules, the localization of GFP-mDia1 to adherens junctions was less pronounced than in non-treated cells (compare Fig. 9B with E) as a significant fraction of GFP-mDia1 was often diffusely distributed across the cytoplasm (Fig. 9E). Nevertheless, even in these conditions, expression of GFP-mDia1 together with RhoA-V14 still significantly enhanced the junctional localization of β-catenin (Fig. 9F) as well as other junctional components (data not shown). Thus, mDia1 activated by Rho

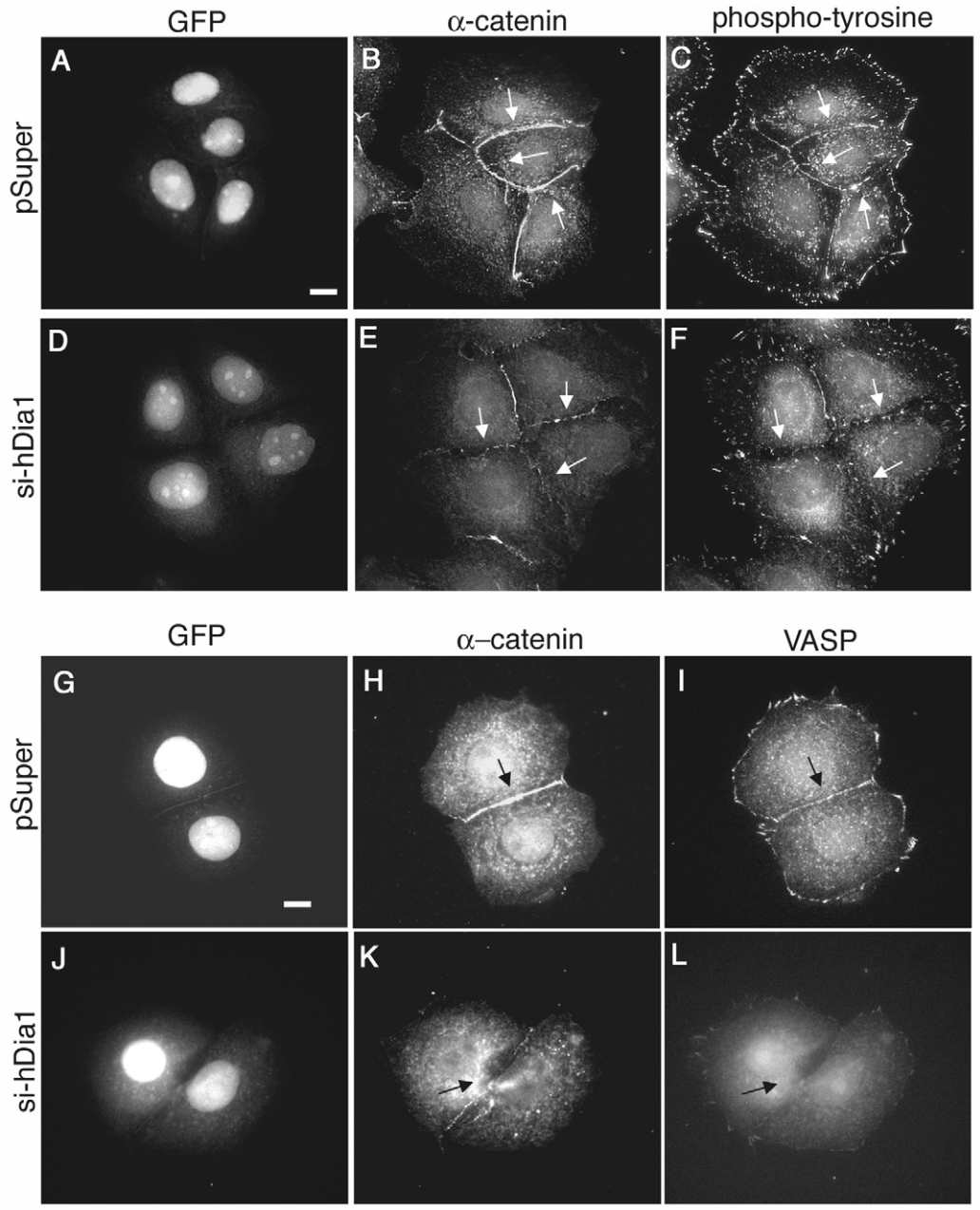

Fig. 5. Effect of Dia1 knockdown on the localization of VASP and phosphotyrosine. Immunofluorescence of cells transfected with a GFP-encoding vector together with either an empty pSuper vector (A-C,G-I) or pSuper si-hDia1 (D-F,J-L) stained with antibodies against α-catenin (B,E,H,K), phospho-tyrosine (C,F) and VASP (I,L). Note that Dia1 deficiency leads to disappearance of these components from the cell-cell interface. Bars, 10 μm. Arrows indicate the contacts between cells.

also strengthens adherens junctions in the absence of microtubules.

The activity of myosin II has been reported to be involved in the formation and maintenance of adherens junctions (Conti et al., 2004; Miyake et al., 2006; Shewan et al., 2005; Yamada and Nelson, 2007). To test the role of myosin II in the Dia1-Rho-induced enhancement of adherens junctions, we treated cells co-transfected with RhoA-V14 and GFP-mDia1 with blebbistatin, a specific inhibitor of nonmuscle myosin II (Straight et al., 2003). Blebbistatin-treated cells experienced the complete disappearance of actin stress fibers (compare Fig. 6E with Fig. 9G). At the same time, a highly exaggerated formation of actin-rich filopodia was observed at the interface between neighboring, contacting cells (Fig. 9G). GFP-mDia1 was mainly localized to these filopodia (Fig. 9H) and was sometimes concentrated in spots at the filopodia tips. Immunofluorescence visualization of E-cadherin revealed its enrichment in these filopodia-like structures at the cell-cell interface (Fig. 9I). Thus, inhibition of myosin II does not interfere with Dia1-induced filopodial activity, but instead blocks the strengthening of adherens junctions in the cells expressing Dia1 together with active RhoA.

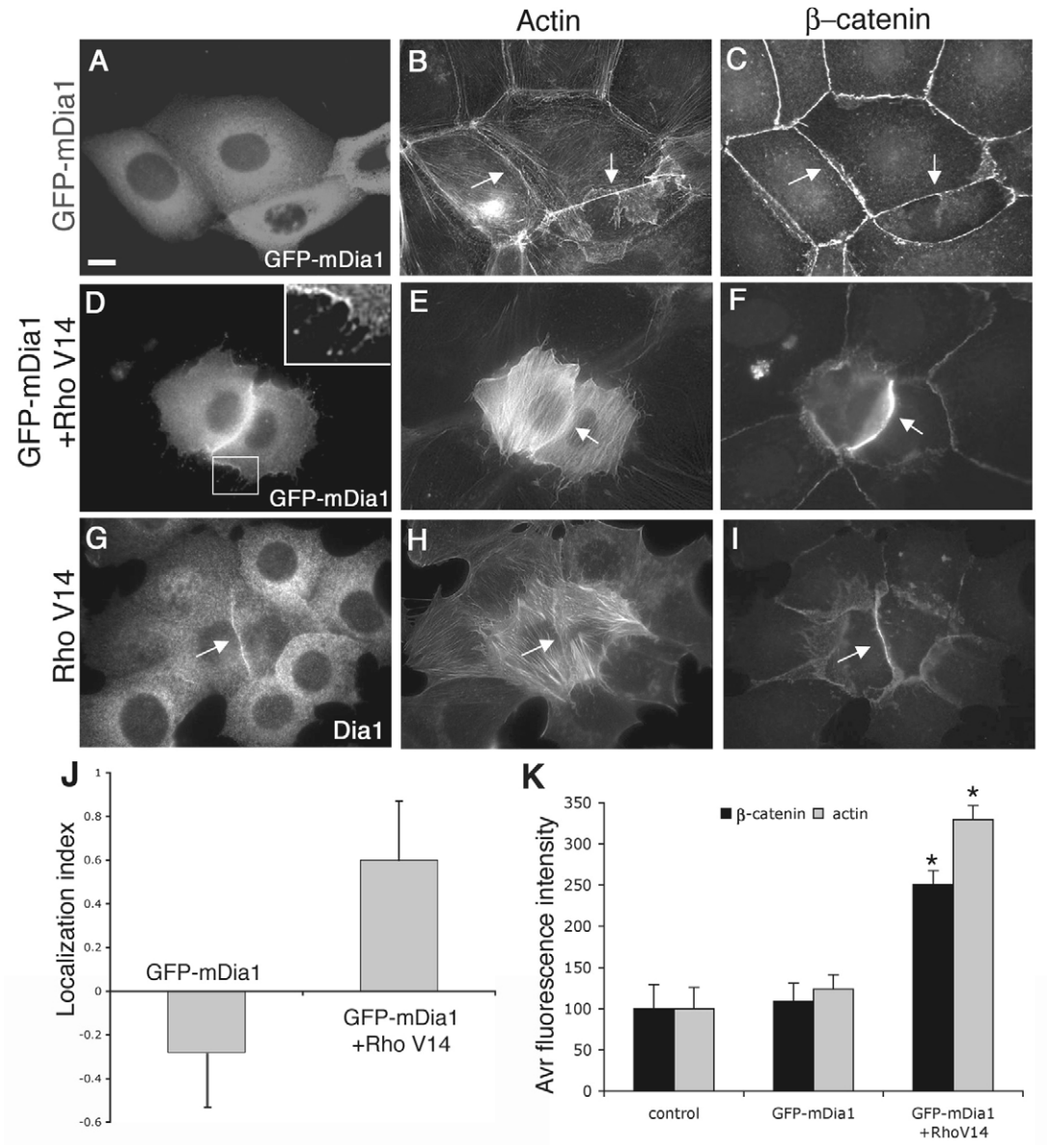

Fig. 6. Dia1 localizes to and strengthens the adherens junctions in a Rho-dependent manner. (A-C) GFP-tagged full-length mDia1 (GFP-mDia1) is distributed diffusely all over the transfected cells (A). The distributions of F-actin (B) and β-catenin (C) in cells expressing GFP-mDia1 are not affected. (D-F) Co-transfection of GFP-mDia1 together with the constitutively active mutant of RhoA (RhoA-V14) leads to a significant enrichment of GFP-mDia1 at cell-cell junctions (D) and formation of numerous filopodia-like projections, with GFP-mDia1 localized to their tips (D, inset). It also promotes formation of prominent phalloidin-stained actin cables (E) and a significant accumulation of β-catenin at the interface between transfected cells (F). (G-I) Transfection of RhoA-V14 strongly enhances the localization of endogenous Dia1 to cell-cell junctions, as revealed by staining with antibodies against Dia1 (G), promotes formation of stress fibers (H) and induces some increase in cell-cell junctions marked by staining for β-catenin (I). Arrows indicate the contacts between cells. (J) Assessment of the Rho-mediated localization of GFP-mDia1 to cell-cell contacts. The fluorescence intensity of GFP-mDia1 was measured by line-scan analysis at cell-cell interfaces. A localization index was calculated as described in Materials and Methods. Means±s.d. are shown. (K) The fluorescence intensities of actin and β-catenin at cell-cell contacts were measured as explained in the legend to Fig. 3. Bars represent the average fluorescence intensity expressed in arbitrary units. Error bars represent s.d. values. Asterisks indicate the values that differ significantly from those of corresponding controls (according to both Kolmogorov-Smirnov (KS) and Student's *t*-test, $P<0.001$). Quantifications were done for three independent experiments, including measurements of 30 pair of cells for each experiment.

Discussion

We found that downregulation of Dia1 in human MCF7 breast carcinoma cells caused adherens junctions to disintegrate. In Dia1-knockdown cells, the levels of the proteins of the cadherin-catenin complex (E-cadherin, α-catenin, β-catenin, etc.) were significantly reduced at the adherens junctions. This effect was especially prominent when both contacting cells lacked Dia1. A normal partner can partially compensate for the deficiency of a knockdown cell; and a similar effect can be seen also when control and E-cadherin-knockdown cells contact

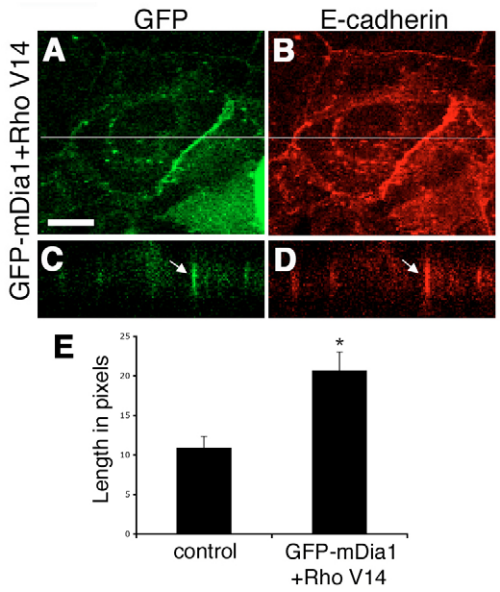

Fig. 7. Activation of exogenous Dia1 leads to increased recruitment of E-cadherin to cell-cell junctions. (A,B) Confocal images of cells co-transfected with both GFP-mDia1- and RhoA-V14-expressing vectors and stained for E-cadherin 20 hours following transfection. A prominent junctional localization of GFP-mDia1 (A) and E-cadherin (B) is evident. (C,D) *XZ* projections of the images (A) and (B), respectively, taken along the white lines. Junctions between transfected cells are indicated by arrows. Bar, 10 μm. (E) Assessment of the width of the 'adhesion belt' in control cells and in cells co-transfected with vectors encoding GFP-mDia1 and RhoA-V14. The lengths of cell-cell contacts at the *XZ* plane are indicated. Quantification was done for 30 pairs of cells for each experiment. Error bars represent s.d. values. The asterisk indicates the value differs significantly from corresponding controls (Student's *t*-test, $P<0.0001$).

each other (Capaldo and Macara, 2007). Intercellular junctions between Dia1-knockdown cells are more sensitive to Ca^{2+} depletion than those between control cells; moreover, a Ca^{2+} switch does not induce formation of proper cell-cell junctions between Dia1-knockdown cells, as revealed by staining with antibodies against E-cadherin and against a marker of tight junctions, cingulin. Before Ca^{2+} depletion, however, some junctions between Dia1-knockdown cells demonstrate a normal localization of cingulin, even when E-cadherin is completely absent. Combined, these results suggest that Dia1 knockdown interferes with the formation and maintenance of E-cadherin-mediated adherens junctions, whereas its effect on the localization of a tight junction protein is secondary.

Dia1 depletion is not accompanied by any decrease in the total amount of E-cadherin or β-catenin. Moreover, Dia1 knockdown in MCF7 cells did not produce severe changes in the overall organization of actin, and this is in agreement with several previous studies analyzing the effects of Dia1 knockdown in other cell types (Hotulainen and Lappalainen, 2006; Yamana et al., 2006). Careful quantification revealed, however, a small but statistically significant decrease of the junctional F-actin levels at the contacts between Dia1-knockdown cells; and the level of the actin-binding protein VASP decreased dramatically. Thus, Dia1 downregulation, most probably, results in a local effect in junctional actin organization rather than a systemic alteration of the whole actin cytoskeleton.

This conclusion is consistent with our observations that active RhoA induces massive translocation of both exogenous GFP-Dia1 and endogenous hDia1 to adherens junctions in MCF7 cells. The mechanism of Dia1 junctional localization, however, seems to be complex. We demonstrated that Dia1 activation by itself is not sufficient for its junctional localization as constitutively active Dia1 variants lacking the N-terminal domain (ΔN1, ΔN2 and ΔN3) fail to localize, whereas Dia1-ΔDAD, which preserves the N-terminal domain, does localize properly. These results are consistent with a recent study (Seth et al., 2006) showing that the N-terminal part of mDia1 is required for its membrane localization.

Interestingly, Dia1-ΔN3 does localize to the junctions if co-transfected with constitutively active RhoA, even though such localization was less prominent than the localization of constructs preserving the N-terminus. Thus, Dia1 localization to the adherens junctions seems to be driven by both N-terminus-dependent and N-terminus-independent interactions. The RhoA-induced localization of the Dia1-ΔN3 variant suggests that, upon activation by RhoA, certain protein(s) might bind Dia1 in an N-terminus-independent manner and so deliver it to the junctions. We hypothesize that the general membrane localization can be driven by an N-terminus-dependent mechanism, as suggested by Seth et al. (Seth et al., 2006), whereas an additional Rho-dependent mechanism drives the specific junctional localization. RhoA itself was reported to be enriched at cell-cell junctions in some experimental situations (Takaishi et al., 1995).

Whatever the mechanism of Dia1 junctional localization, the fact that such localization significantly enhances the junctions is most interesting. Indeed, recruitment of high levels of F-actin and bona fide adherens junction proteins into junctions between cells expressing GFP-mDia1 together with Rho-V14 even causes an increase in the width of the adhesion belt, as revealed by confocal microscopy. It is worth noting that the general reorganization of the actin cytoskeleton observed in these cells (development of numerous parallel actin filament bundles) is not sufficient for the enhancement of adherens junctions by itself. Augmented formation of actin bundles can be observed upon expression of constitutively active Dia1 lacking the N-terminal domain, and therefore nonlocalized to the junctions, or even by expression of active RhoA-V14 in the condition of Dia1 knockdown. In both cases, the formation of prominent actin bundles is not accompanied by enhancement of adherens junctions. Thus, the effect of Dia1 activation on adherens junctions (similar to the effect of Dia1 knockdown) is not a consequence of gross changes in actin polymerization, rather a result of local actin reorganization at the junctional areas.

Although the best-documented activities of Dia1 are the enhancement of actin nucleation and elongation (Kovar et al., 2006; Li and Higgs, 2003; Moseley et al., 2004; Romero et al., 2004), several in vivo studies suggest that Dia1 also affects microtubule stability and co-alignment (Goulimari et al., 2005; Ishizaki et al., 2001; Palazzo et al., 2001). We checked whether the stimulatory effect of Dia1 on adherens junctions depended on microtubules. We have shown that prolonged incubation

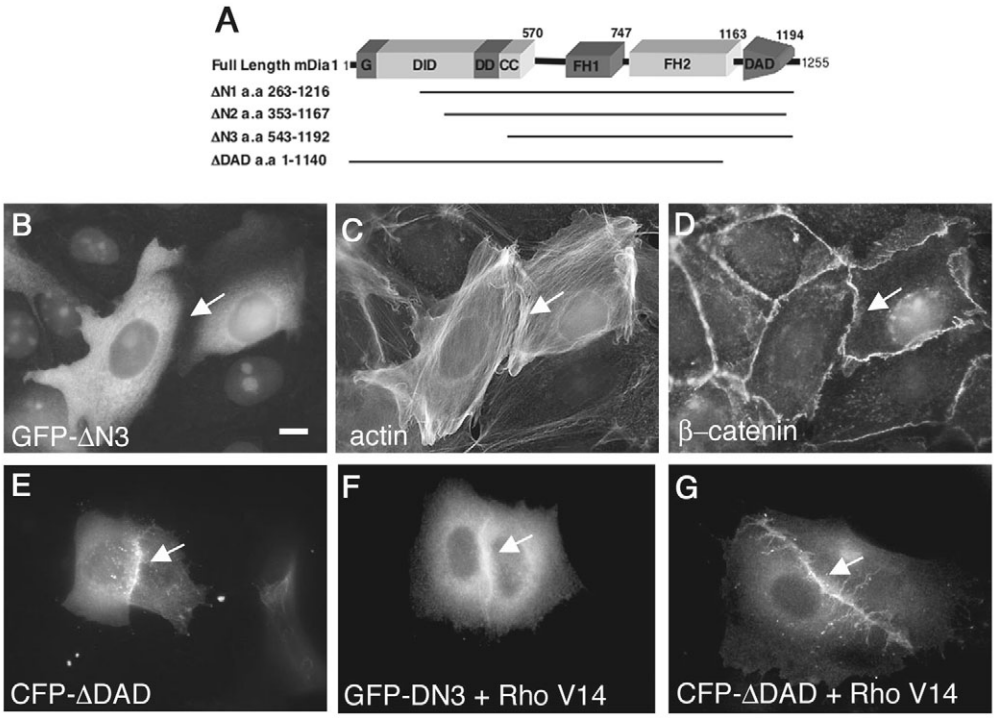

Fig. 8. Localization of Dia1 and truncated mutant Dia1 proteins. (A) Structures of full-length mDia1 and its constitutively active mutants that were used in this study. The black lines indicate the region encoded by each mutant. The numbers correspond to the amino acid positions in the mDia1 sequence. None of the mutants contains an intact C-terminus. Only the CFP-ΔDAD mutant preserves the N-terminal domain in its entirety. (B) Diffuse distribution of the Dia1 mutant GFP-ΔN3 and staining of actin (C) and β-catenin (D) in the corresponding cells. (E) Junctional localization of the Dia1 mutant CFP-ΔDAD. (F) Co-transfection of GFP-ΔN3 together with a vector encoding RhoA-V14 promotes the localization of the Dia1 mutant GFP-ΔN3 to cell-cell junctions. (G) Cells expressing the mutant CFP-ΔDAD co-transfected together with RhoA-V14 display a prominent mDia1-ΔDAD localization to cell-cell junctions (as well as to tips of filopodia). Arrows indicate cell-cell junctions. Bar, 10 μm.

with a microtubule-disrupting drug did indeed reduce (but did not entirely abolish) localization of Rho-activated mDia1 to the adherens junctions; the mechanism of this interesting effect certainly warrants further investigation. At the same time, microtubule disruption did not prevent augmentation of adherens junctions upon overexpression of mDia1 and Rho-V14. Therefore, these results do not exclude the idea that microtubules play some role in the delivery of Dia1 to the adherens junctions, but they do show that Dia1 does not affect adherens junctions by means of an involvement with microtubules.

However, the formation of Dia1-driven mature adherens junctions clearly requires the activity of myosin II. Although evidence for the involvement of myosin in the regulation of adherens junctions was found previously (Conti et al., 2004; Grosheva et al., 2006; Miyake et al., 2006; Shewan et al., 2005; Yamada and Nelson, 2007), the effect of myosin II inhibition we observed in our system (production of filopodia in the cell-cell junction area, instead of junction enhancement) was dramatic. It is possible that two pathways downstream of RhoA cooperate to induce junction maturation: one inducing actin polymerization by means of Dia1 and another inducing activation of myosin II by means of Rho kinase.

Several mechanisms based on Dia1-mediated local actin polymerization could potentially be important for the formation and maintenance of cadherin-mediated adhesions. The apparent stimulation of formation of filopodia by active mDia1, which resembles the well-documented effects of its homolog Dia2 (Pellegrin and Mellor, 2005; Peng et al., 2003; Schirenbeck et al., 2005; Wallar et al., 2006), might play a role at the early stages of adhesion, when contacts made through filopodia-like projections are important (Vasioukhin et al., 2000). It is worth noting that the formation of Dia1-induced filopodia occurred mainly at the interface between contacting cells, whereas few filopodia were directed to the substratum. The mechanism of such selectivity deserves further investigation.

Our experiments with inhibition of the activity of myosin II allowed the dissection of the two stages of Dia1-mediated adherens junction strengthening: the formation of filopodia, which is preserved or even exaggerated in conditions of myosin II inhibition, and the formation of mature linear junctions, for which cooperation with myosin II is required. The predicted ability of formins and, in particular, Dia1 to enhance actin polymerization upon application of mechanical force (Kozlov and Bershadsky, 2004) could play a role in the processes of myosin-II-driven force-induced assembly of cadherin adhesions.

At the later stages of assembly, a submembranous sheet of Dia1-nucleated actin filaments could increase adhesion by reducing the lateral mobility of cadherin receptors in the plane of the membrane; this mechanism does not require a direct link

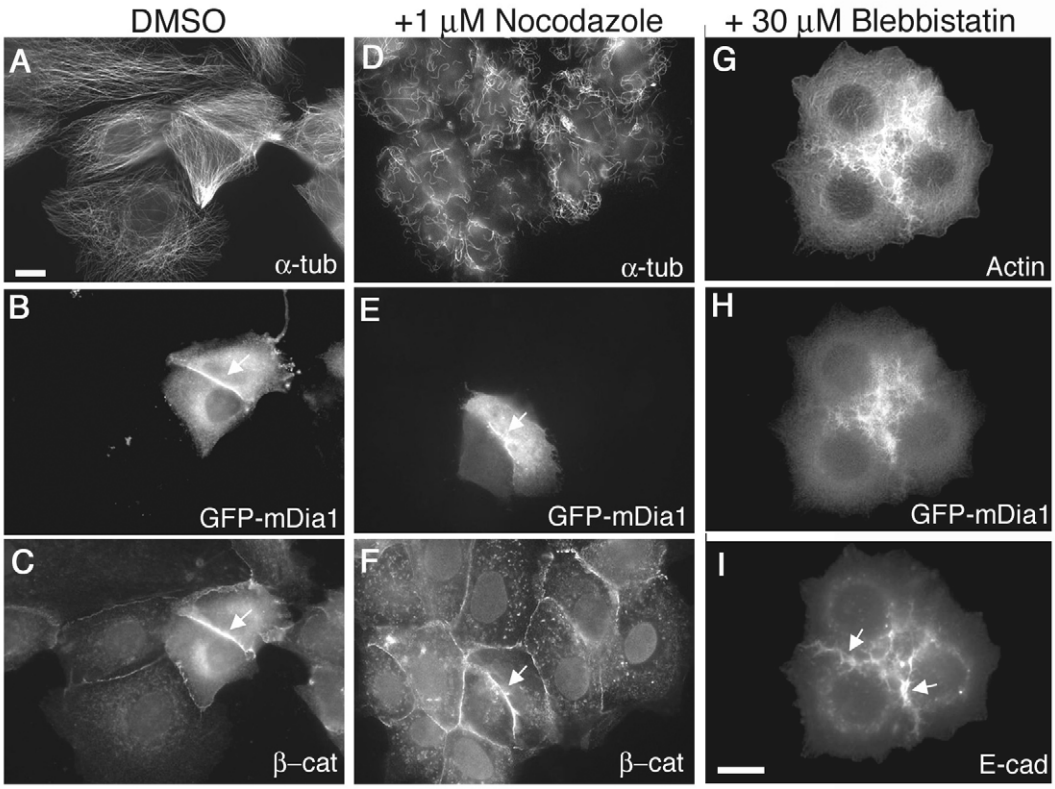

Fig. 9. Inhibition of myosin II but not disruption of microtubules alters the Dia1-induced morphology of adherens junctions. (A-I) MCF7 cells transfected with GFP-mDia1 together with a vector encoding RhoA-V14. Cells were treated with DMSO (A-C) or 1 μM nocodazole (D-F) for 24 hours. The drugs were added 4 hours following transfection. Cells were stained for β-catenin (C,F) and α-tubulin (A,D). Cells with intact microtubules (A) display a localization of GFP-mDia1 at cell-cell junctions (B) and a significant recruitment of β-catenin to the cell-cell junctions of transfected cells, as revealed by staining (C). Cells treated with nocodazole show disrupted microtubule networks (D) and a higher cytoplasmic level of GFP-mDia1, even though GFP-mDia1 still was preferentially localized to the adherens junctions (E). Disruption of the microtubule networks did not prevent, however, the increase of the recruitment of β-catenin to the junctions between transfected cells (F), as compared with their non-transfected neighbors. (G-I) Cells were treated with 30 μM blebbistatin for 6 hours preceding fixation and staining with phalloidin (G) and an antibody against E-cadherin (I). GFP-mDia1 localizes to the filopodia in transfected cells (H). Arrows indicate cell-cell junctions. Bars, 10 μm.

between cadherin receptors and the actin filaments (Baumgartner et al., 2003; Iino et al., 2001; Sako et al., 1998). Another interesting possibility is the actin-polymerization-dependent control of turnover of adhesion receptors. For example, modulation of the organization of submembranous actin might protect cadherin from endocytosis, and this could be a very important pathway of adhesion regulation (Ivanov et al., 2004; Le et al., 1999; Troyanovsky et al., 2006).

Finally, future studies are required to verify and elucidate the proposed Dia1-dependent mechanisms, as well as investigate the relationship between Dia1 and other factors affecting actin polymerization in the regulation of the assembly of cell-cell adhesions. Even though the Arp2/3 complex (Kovacs et al., 2002; Verma et al., 2004), WAVE (Yamazaki et al., 2006), N-WASP (Ivanov et al., 2005), cortactin (El Sayegh et al., 2004; Helwani et al., 2004), VASP (Scott et al., 2006; Vasioukhin et al., 2000), formin-1 (Kobielak et al., 2004) and Dia1 (this study) are all involved in the regulation of adherens junctions, the roles of these proteins probably do not overlap entirely. For example, the prominent and unique phenotypes observed upon Dia1 knockdown and Dia1 activation are indicative of the specific and nonredundant functions of this protein in the control of cell-cell adhesion. Dia1-dependent regulation represents a novel facet in the crosstalk between the functions of the cytoskeleton and cadherins.

Materials and Methods

Cells and reagents

MCF7 cells were cultured in Dulbecco's modified Eagle's medium supplemented with antibiotics, 2 mM glutamine (Gibco, Rhenium, Jerusalem, Israel) and 10% heat-inactivated fetal calf serum (Biological Industries, Kibbutz Beit Haemek, Israel) at 37°C in a 5% CO_2 humidified atmosphere. Cells were replated using standard trypsin-EDTA solution. Nocodazole was obtained from Sigma-Aldrich (St Louis, MO), and blebbistatin [(±)-1-phenyl-1,2,3,4-tetrahydro-4-hydroxypyrrolo[2,3-b]-7-methylquinolin-4-one] from Calbiochem (San Diego, CA). Both reagents were added to the growth medium from stock solutions in DMSO, so that final the concentration of DMSO in solution did not exceed 0.06%. Calcium-depletion experiments were performed in calcium-magnesium-free Hanks balanced salt solution (Sigma-Aldrich) containing 4 mM EGTA. After 15 minutes, the EGTA-containing HBSS was replaced with calcium-containing DMEM, and reconstitution of cell-cell contacts was monitored for up to 2 hours.

Plasmids and transfection

The pSuper Dia1-shRNA (called here si-hDia1), the pSuper-retro-Dia1-shRNA and the pSuper-retro-LacZ vectors were kindly provided to us by Y. Ziv and Y. Shiloh (Sackler School of Medicine, Tel Aviv University, Israel). Briefly, a small interfering oligonucleotide specific for human Dia1 and corresponding to its sequence from base 707 to 725 (GCATGAGATCATTCGCTGC) was synthesized, annealed and cloned in the pSuper plasmids (Brummelkamp et al., 2002). The sequence was then

verified by DNA sequencing. The plasmids encoding GFP-fused full-length mDia1 (GFP-mDia1), as well as its constitutively active truncated mutants mDia1-ΔN1, mDia1-ΔN2 and mDia1-ΔN3 described previously (Watanabe et al., 1999), were kindly provided by S. Narumiya (Faculty of Medicine, Kyoto University, Japan). The CFP-ΔDAD truncated mutant lacking the DAD domain (residues 1-1140) (Fig. 7A) was derived from the GFP-mDia1 construct by PCR and ligated into *Sal*I/*Bgl*II in the vector pECFP-C1 (BD Biosciences).

Transient transfections were carried out in six-well plates by DreamFect reagent (Oz Biosciences, Parc scientifique de Luminy, Marseille CEDEX 9, France) according to the manufacturer's instructions. The ratio between si-hDia1 plasmid and pGFP-C1 was 3:1. Four hours later, the cells were replated onto 13 mm round coverslips or glass-bottomed culture dishes (MaTek, Ashland, MA) pre-coated with 10 μg/ml fibronectin (tissue-culture grade, Sigma-Aldrich).

To assess the hDia1 expression, cells transfected with pGFP-C1 and empty pSuper plasmids (control) or pGFP-C1 and pSuper-siDia1 plasmids were collected by FACS sorting 48-72 hours following transfection and lysed. A mouse monoclonal antibody (mAb) against p140mDia1 and a mouse mAb against tubulin (Sigma-Aldrich) were used for western blotting.

An MCF7 si-hDia1 stable cell line was obtained by transfection with the pSuper-retro-shDia1 plasmid (the Dia1-shRNA sequence was the same as for the transient transfection). pSuper-retro-LacZ plasmid, bearing an irrelevant shRNA against the LacZ operon, was used as a control. Selection was conducted in the presence of 0.4 μg/ml puromycin (Sigma-Aldrich) for 10 days. Cell lysates were prepared and checked by western blot, which showed an ~90% reduction of mDia1 protein. Tubulin was used as a loading control. Quantification of western blot signals was performed using the ImageJ software.

Immunostaining, microscopy and data analysis

Cells processed for immunostaining were fixed and permeabilized 48-72 hours after transfection by incubation for 3 minutes in 3.7% paraformaldehyde (PFA) with 0.5% Triton X-100, followed by PBS washing and incubation in 3.7% PFA at room temperature for an additional 30 minutes. For microtubule immunostaining, fixation with a solution containing 3% paraformaldehyde, 0.05% glutaraldehyde and 0.25% Triton X-100 was used. Cells were immunostained by sequential incubation with the primary and secondary antibodies, for one hour each. After washing with PBS, cells were mounted in Elvanol (Mowiol 4-88, Hoechst, Frankfurt, Germany).

The following primary antibodies were used for staining: mouse mAb against p140mDia1 (BD Biosciences, Heidelberg, Germany); mouse mAb against human E-cadherin (BD Biosciences); rabbit polyclonal anti-β- and α-catenins and monoclonal anti-α-tubulin, clone DM1A (Sigma-Aldrich); mouse mAb against VASP kindly provided by Jurgen Wehland (Helmholtz Centre for Infection Research, Braunschweig, Germany); mouse mAb against phosphotyrosine (clone 4G10, Upstate Biotechnology); and a rabbit polyclonal antibody against cingulin, a gift of Sandra Citi (Dept of Molecular Biology, University of Geneva, Switzerland). The secondary antibodies used were: goat anti-mouse or anti-rabbit, conjugated to Cy3, Cy5 or Alexa 488 fluorochromes (Jackson Laboratories, West Grove, PA). F-Actin was visualized using a coumarin-phalloidin probe (Small et al., 1988) obtained from Sigma-Aldrich.

Images of fixed cells were recorded using the DeltaVision System (Applied Precision, Issaquah, WA) that included an Olympus IX71 inverted microscope equipped with a CoolSnap HQ camera (Photometrics, Tucson, AZ), a 100 W mercury lamp and excitation and emission filter wheels. Images were acquired with an Olympus plan ApoN 60× 1.42 N/A objective.

Laser-scanning confocal microscopy (LSCM) was performed using a Radiant 2000 laser scanning system operated in conjunction with an Eclipse TLE300 inverted microscope (Nikon Corporation, Tokyo, Japan) equipped with a 63× oil-immersion objective, running under Bio-Rad software (Bio-Rad Laboratories, Hercules, CA). Serial *XY* optical sections were recorded and *XZ* and *YZ* profiles were produced using the Bio-Rad software package. Contrast adjustment of raw images was performed in Adobe Photoshop 7 or ImageJ. Panels were assembled in Adobe Photoshop 7.

The integrity of the adherens junctions was quantified by estimation of the fraction of cell-cell contacts preserving intact, non-disturbed E-cadherin-positive junctions. A contact between two cells was considered preserved when the total length of a continuous E-cadherin-positive line was at least 50% of the distance between the corresponding vertices of the cell. ImageJ software was used for the length measurements. Quantitative assessment of adherens junction integrity in Dia1-knockdown cells was performed in three individual experiments by measuring 30 pairs of cells for each case considered.

Levels of E-cadherin, β-catenin, actin and GFP fluorescence intensity at cell-cell junctions were quantified using the line-scan tool in MetaMorph software (Molecular Devices Corporation, Sunnyvale, CA). Intensity measurements were performed along segments oriented perpendicular to the contact, as described by Verma and colleagues (Verma et al., 2004). Intensity profiles (Fig. 3C,D) were calculated by averaging the segments covering a square measuring 20×20 pixels. Between 2 to 5 of such squares per contact were measured in order to cover the entire contact length. The peak pixel intensity values were taken as the measure of fluorescence intensity at the contact (see Results); for the quantification of GFP localization at the junction, we introduced a localization index (I). To calculate this, we subtracted the highest value of cytoplasmic intensity (C) from the peak value of intensity at the junction (J) and divided this difference by the cytoplasmic intensity C, such that: I=(J–C)/C. About 30 contacts were analyzed per experiment, and each experiment was repeated three times.

We are grateful to Y. Shiloh and Y. Ziv (Sackler School of Medicine, Tel Aviv University, Israel) and to S. Narumiya (Faculty of Medicine, Kyoto University, Kyoto, Japan) for providing plasmids, and to Sandra Citi (Department of Molecular Biology, University of Geneva, Switzerland) for the antibody to cingulin. We thank Miri Lev Ran for technical assistance and Mike Grant and Lisa Rogers for critically reading the manuscript. L.C. was supported by a S. Lombroso Fellowship for Cancer Research. C.B. was supported by the Wellcome Centre core award 077100. This study was funded in part by grants from the Israel Sciences Foundation, Minerva Foundation and Pasteur-Weizmann Council to A.D.B. A.D.B. holds the Joseph Moss Professorial Chair in Biomedical Research.

References

Angres, B., Barth, A. and Nelson, W. J. (1996). Mechanism for transition from initial to stable cell-cell adhesion: kinetic analysis of E-cadherin-mediated adhesion using a quantitative adhesion assay. *J. Cell Biol.* **134**, 549-557.

Baumgartner, W., Schutz, G. J., Wiegand, J., Golenhofen, N. and Drenckhahn, D. (2003). Cadherin function probed by laser tweezer and single molecule fluorescence in vascular endothelial cells. *J. Cell Sci.* **116**, 1001-1011.

Bershadsky, A. (2004). Magic touch: how does cell-cell adhesion trigger actin assembly? *Trends Cell Biol.* **14**, 589-593.

Boguslavsky, S., Grosheva, I., Landau, E., Cohen, M., Arnold, K., Shtutman, M., Feinstein, E., Geiger, B. and Bershadsky, A. (2007). p120 catenin regulates lamellipodial dynamics and cell adhesion in cooperation with cortactin. *Proc. Natl. Acad. Sci. USA* **104**, 10882-10887.

Braga, V. M. (2002). Cell-cell adhesion and signalling. *Curr. Opin. Cell Biol.* **14**, 546-556.

Braga, V. M., Machesky, L. M., Hall, A. and Hotchin, N. A. (1997). The small GTPases Rho and Rac are required for the establishment of cadherin-dependent cell-cell contacts. *J. Cell Biol.* **137**, 1421-1431.

Brummelkamp, T. R., Bernards, R. and Agami, R. (2002). A system for stable expression of short interfering RNAs in mammalian cells. *Science* **296**, 550-553.

Capaldo, C. T. and Macara, I. G. (2007). Depletion of E-cadherin disrupts establishment but not maintenance of cell junctions in Madin-Darby canine kidney epithelial cells. *Mol. Biol. Cell* **18**, 189-200.

Chu, Y. S., Thomas, W. A., Eder, O., Pincet, F., Perez, E., Thiery, J. P. and Dufour, S. (2004). Force measurements in E-cadherin-mediated cell doublets reveal rapid adhesion strengthened by actin cytoskeleton remodeling through Rac and Cdc42. *J. Cell Biol.* **167**, 1183-1194.

Citi, S., Sabanay, H., Jakes, R., Geiger, B. and Kendrick-Jones, J. (1988). Cingulin, a new peripheral component of tight junctions. *Nature* **333**, 272-276.

Conti, M. A., Even-Ram, S., Liu, C., Yamada, K. M. and Adelstein, R. S. (2004). Defects in cell adhesion and the visceral endoderm following ablation of nonmuscle myosin heavy chain II-A in mice. *J. Biol. Chem.* **279**, 41263-41266.

El Sayegh, T. Y., Arora, P. D., Laschinger, C. A., Lee, W., Morrison, C., Overall, C. M., Kapus, A. and McCulloch, C. A. (2004). Cortactin associates with N-cadherin adhesions and mediates intercellular adhesion strengthening in fibroblasts. *J. Cell Sci.* **117**, 5117-5131.

Faix, J. and Grosse, R. (2006). Staying in shape with formins. *Dev. Cell* **10**, 693-706.

Goode, B. L. and Eck, M. J. (2007). Mechanism and function of formins in the control of actin assembly. *Annu. Rev. Biochem.* **76**, 593-627.

Goulimari, P., Kitzing, T. M., Knieling, H., Brandt, D. T., Offermanns, S. and Grosse, R. (2005). Galpha12/13 is essential for directed cell migration and localized Rho-Dia1 function. *J. Biol. Chem.* **280**, 42242-42251.

Grosheva, I., Vittitow, J. L., Goichberg, P., Gabelt, B. T., Kaufman, P. L., Borras, T., Geiger, B. and Bershadsky, A. D. (2006). Caldesmon effects on the actin cytoskeleton and cell adhesion in cultured HTM cells. *Exp. Eye Res.* **82**, 945-958.

Gumbiner, B. M. (2005). Regulation of cadherin-mediated adhesion in morphogenesis. *Nat. Rev. Mol. Cell Biol.* **6**, 622-634.

Helwani, F. M., Kovacs, E. M., Paterson, A. D., Verma, S., Ali, R. G., Fanning, A. S., Weed, S. A. and Yap, A. S. (2004). Cortactin is necessary for E-cadherin-mediated contact formation and actin reorganization. *J. Cell Biol.* **164**, 899-910.

Higgs, H. N. (2005). Formin proteins: a domain-based approach. *Trends Biochem. Sci.* **30**, 342-353.

Higgs, H. N. and Pollard, T. D. (2001). Regulation of actin filament network formation through ARP2/3 complex: activation by a diverse array of proteins. *Annu. Rev. Biochem.* **70**, 649-676.

Hotulainen, P. and Lappalainen, P. (2006). Stress fibers are generated by two distinct actin assembly mechanisms in motile cells. *J. Cell Biol.* **173**, 383-394.

Iino, R., Koyama, I. and Kusumi, A. (2001). Single molecule imaging of green fluorescent proteins in living cells: E-cadherin forms oligomers on the free cell surface. *Biophys. J.* **80**, 2667-2677.

Ishizaki, T., Morishima, Y., Okamoto, M., Furuyashiki, T., Kato, T. and Narumiya, S. (2001). Coordination of microtubules and the actin cytoskeleton by the Rho effector mDia1. *Nat. Cell Biol.* **3**, 8-14.

Ivanov, A. I., Nusrat, A. and Parkos, C. A. (2004). Endocytosis of epithelial apical junctional proteins by a clathrin-mediated pathway into a unique storage compartment. *Mol. Biol. Cell* **15**, 176-188.

Ivanov, A. I., Hunt, D., Utech, M., Nusrat, A. and Parkos, C. A. (2005). Differential roles for actin polymerization and a myosin II motor in assembly of the epithelial apical junctional complex. *Mol. Biol. Cell* **16**, 2636-2650.

Ivanov, A. I., McCall, I. C., Babbin, B., Samarin, S. N., Nusrat, A. and Parkos, C. A. (2006). Microtubules regulate disassembly of epithelial apical junctions. *BMC Cell Biol.* **7**, 12.

Kobielak, A., Pasolli, H. A. and Fuchs, E. (2004). Mammalian formin-1 participates in adherens junctions and polymerization of linear actin cables. *Nat. Cell Biol.* **6**, 21-30.

Kovacs, E. M., Goodwin, M., Ali, R. G., Paterson, A. D. and Yap, A. S. (2002). Cadherin-directed actin assembly: E-cadherin physically associates with the Arp2/3 complex to direct actin assembly in nascent adhesive contacts. *Curr. Biol.* **12**, 379-382.

Kovar, D. R., Harris, E. S., Mahaffy, R., Higgs, H. N. and Pollard, T. D. (2006). Control of the assembly of ATP- and ADP-actin by formins and profilin. *Cell* **124**, 423-435.

Kozlov, M. M. and Bershadsky, A. D. (2004). Processive capping by formin suggests a force-driven mechanism of actin polymerization. *J. Cell Biol.* **167**, 1011-1017.

Kraemer, A., Goodwin, M., Verma, S., Yap, A. S. and Ali, R. G. (2007). Rac is a dominant regulator of cadherin-directed actin assembly that is activated by adhesive ligation independently of Tiam1. *Am. J. Physiol. Cell Physiol.* **292**, C1061-C1069.

Le, T. L., Yap, A. S. and Stow, J. L. (1999). Recycling of E-cadherin: a potential mechanism for regulating cadherin dynamics. *J. Cell Biol.* **146**, 219-232.

Li, F. and Higgs, H. N. (2003). The mouse Formin mDia1 is a potent actin nucleation factor regulated by autoinhibition. *Curr. Biol.* **13**, 1335-1340.

Mary, S., Charrasse, S., Meriane, M., Comunale, F., Travo, P., Blangy, A. and Gauthier-Rouviere, C. (2002). Biogenesis of N-cadherin-dependent cell-cell contacts in living fibroblasts is a microtubule-dependent kinesin-driven mechanism. *Mol. Biol. Cell* **13**, 285-301.

Mege, R. M., Gavard, J. and Lambert, M. (2006). Regulation of cell-cell junctions by the cytoskeleton. *Curr. Opin. Cell Biol.* **18**, 541-548.

Miyake, Y., Inoue, N., Nishimura, K., Kinoshita, N., Hosoya, H. and Yonemura, S. (2006). Actomyosin tension is required for correct recruitment of adherens junction components and zonula occludens formation. *Exp. Cell Res.* **312**, 1637-1650.

Moseley, J. B., Sagot, I., Manning, A. L., Xu, Y., Eck, M. J., Pellman, D. and Goode, B. L. (2004). A conserved mechanism for Bni1- and mDia1-induced actin assembly and dual regulation of Bni1 by Bud6 and profilin. *Mol. Biol. Cell* **15**, 896-907.

Nicholson-Dykstra, S., Higgs, H. N. and Harris, E. S. (2005). Actin dynamics: growth from dendritic branches. *Curr. Biol.* **15**, R346-R357.

Olson, M. F. (2003). Dispatch. GTPase signalling: new functions for Diaphanous-related formins. *Curr. Biol.* **13**, R360-R362.

Otomo, T., Otomo, C., Tomchick, D. R., Machius, M. and Rosen, M. K. (2005). Structural basis of Rho GTPase-mediated activation of the formin mDia1. *Mol. Cell* **18**, 273-281.

Palazzo, A. F., Cook, T. A., Alberts, A. S. and Gundersen, G. G. (2001). mDia mediates Rho-regulated formation and orientation of stable microtubules. *Nat. Cell Biol.* **3**, 723-729.

Pellegrin, S. and Mellor, H. (2005). The Rho family GTPase Rif induces filopodia through mDia2. *Curr. Biol.* **15**, 129-133.

Peng, J., Wallar, B. J., Flanders, A., Swiatek, P. J. and Alberts, A. S. (2003). Disruption of the Diaphanous-related formin Drf1 gene encoding mDia1 reveals a role for Drf3 as an effector for Cdc42. *Curr. Biol.* **13**, 534-545.

Perez-Moreno, M. and Fuchs, E. (2006). Catenins: keeping cells from getting their signals crossed. *Dev. Cell* **11**, 601-612.

Reynolds, A. B. (2007). p120-catenin: past and present. *Biochim. Biophys. Acta* **1773**, 2-7.

Romero, S., Le Clainche, C., Didry, D., Egile, C., Pantaloni, D. and Carlier, M. F. (2004). Formin is a processive motor that requires profilin to accelerate actin assembly and associated ATP hydrolysis. *Cell* **119**, 419-429.

Rose, R., Weyand, M., Lammers, M., Ishizaki, T., Ahmadian, M. R. and Wittinghofer, A. (2005). Structural and mechanistic insights into the interaction between Rho and mammalian Dia. *Nature* **435**, 513-518.

Sahai, E. and Marshall, C. J. (2002). ROCK and Dia have opposing effects on adherens junctions downstream of Rho. *Nat. Cell Biol.* **4**, 408-415.

Sako, Y., Nagafuchi, A., Tsukita, S., Takeichi, M. and Kusumi, A. (1998). Cytoplasmic regulation of the movement of E-cadherin on the free cell surface as studied by optical tweezers and single particle tracking: corralling and tethering by the membrane skeleton. *J. Cell Biol.* **140**, 1227-1240.

Sallee, J. L., Wittchen, E. S. and Burridge, K. (2006). Regulation of cell adhesion by protein-tyrosine phosphatases: II. Cell-cell adhesion. *J. Biol. Chem.* **281**, 16189-16192.

Schirenbeck, A., Bretschneider, T., Arasada, R., Schleicher, M. and Faix, J. (2005). The Diaphanous-related formin dDia2 is required for the formation and maintenance of filopodia. *Nat. Cell Biol.* **7**, 619-625.

Scott, J. A., Shewan, A. M., den Elzen, N. R., Loureiro, J. J., Gertler, F. B. and Yap, A. S. (2006). Ena/VASP proteins can regulate distinct modes of actin organization at cadherin-adhesive contacts. *Mol. Biol. Cell* **17**, 1085-1095.

Seth, A., Otomo, C. and Rosen, M. K. (2006). Autoinhibition regulates cellular localization and actin assembly activity of the diaphanous-related formins FRLalpha and mDia1. *J. Cell Biol.* **174**, 701-713.

Shewan, A. M., Maddugoda, M., Kraemer, A., Stehbens, S. J., Verma, S., Kovacs, E. M. and Yap, A. S. (2005). Myosin 2 is a key Rho kinase target necessary for the local concentration of E-cadherin at cell-cell contacts. *Mol. Biol. Cell* **16**, 4531-4542.

Small, J. V., Zobeley, S., Rinnerthaler, G. and Faulstich, H. (1988). Coumarin-phalloidin: a new actin probe permitting triple immunofluorescence microscopy of the cytoskeleton. *J. Cell Sci.* **89**, 21-24.

Stehbens, S. J., Paterson, A. D., Crampton, M. S., Shewan, A. M., Ferguson, C., Akhmanova, A., Parton, R. G. and Yap, A. S. (2006). Dynamic microtubules regulate the local concentration of E-cadherin at cell-cell contacts. *J. Cell Sci.* **119**, 1801-1811.

Straight, A. F., Cheung, A., Limouze, J., Chen, I., Westwood, N. J., Sellers, J. R. and Mitchison, T. J. (2003). Dissecting temporal and spatial control of cytokinesis with a myosin II Inhibitor. *Science* **299**, 1743-1747.

Takaishi, K., Sasaki, T., Kameyama, T., Tsukita, S., Tsukita, S. and Takai, Y. (1995). Translocation of activated Rho from the cytoplasm to membrane ruffling area, cell-cell adhesion sites and cleavage furrows. *Oncogene* **11**, 39-48.

Tominaga, T., Sahai, E., Chardin, P., McCormick, F., Courtneidge, S. A. and Alberts, A. S. (2000). Diaphanous-related formins bridge Rho GTPase and Src tyrosine kinase signaling. *Mol. Cell* **5**, 13-25.

Troyanovsky, R. B., Sokolov, E. P. and Troyanovsky, S. M. (2006). Endocytosis of cadherin from intracellular junctions is the driving force for cadherin adhesive dimer disassembly. *Mol. Biol. Cell* **17**, 3484-3493.

van Deurs, B., Zou, Z. Z., Briand, P., Balslev, Y., Petersen, O. W. (1987). Epithelial membrane polarity: a stable, differentiated feature of an established human breast carcinoma cell line MCF-7. *J. Histochem. Cytochem.* **35**, 461-469.

Vasioukhin, V., Bauer, C., Yin, M. and Fuchs, E. (2000). Directed actin polymerization is the driving force for epithelial cell-cell adhesion. *Cell* **100**, 209-219.

Verma, S., Shewan, A. M., Scott, J. A., Helwani, F. M., den Elzen, N. R., Miki, H., Takenawa, T. and Yap, A. S. (2004). Arp2/3 activity is necessary for efficient formation of E-cadherin adhesive contacts. *J. Biol. Chem.* **279**, 34062-34070.

Volberg, T., Geiger, B., Dror, R. and Zick, Y. (1991). Modulation of intercellular adherens-type junctions and tyrosine phosphorylation of their components in RSV-transformed cultured chick lens cells. *Cell Regul.* **2**, 105-120.

Wallar, B. J., Stropich, B. N., Schoenherr, J. A., Holman, H. A., Kitchen, S. M. and Alberts, A. S. (2006). The basic region of the diaphanous-autoregulatory domain (DAD) is required for autoregulatory interactions with the diaphanous-related formin inhibitory domain. *J. Biol. Chem.* **281**, 4300-4307.

Watanabe, N., Madaule, P., Reid, T., Ishizaki, T., Watanabe, G., Kakizuka, A., Saito, Y., Nakao, K., Jockusch, B. M. and Narumiya, S. (1997). p140mDia, a mammalian homolog of Drosophila diaphanous, is a target protein for Rho small GTPase and is a ligand for profilin. *EMBO J.* **16**, 3044-3056.

Watanabe, N., Kato, T., Fujita, A., Ishizaki, T. and Narumiya, S. (1999). Cooperation between mDia1 and ROCK in Rho-induced actin reorganization. *Nat. Cell Biol.* **1**, 136-143.

Waterman-Storer, C. M., Salmon, W. C. and Salmon, E. D. (2000). Feedback interactions between cell-cell adherens junctions and cytoskeletal dynamics in newt lung epithelial cells. *Mol. Biol. Cell* **11**, 2471-2483.

Weis, W. I. and Nelson, W. J. (2006). Re-solving the cadherin-catenin-actin conundrum. *J. Biol. Chem.* **281**, 35593-35597.

Wheelock, M. J. and Johnson, K. R. (2003). Cadherins as modulators of cellular phenotype. *Annu. Rev. Cell Dev. Biol.* **19**, 207-235.

Yamada, S. and Nelson, W. J. (2007). Localized zones of Rho and Rac activities drive initiation and expansion of epithelial cell cell adhesion. *J. Cell Biol.* **178**, 517-527.

Yamana, N., Arakawa, Y., Nishino, T., Kurokawa, K., Tanji, M., Itoh, R. E., Monypenny, J., Ishizaki, T., Bito, H., Nozaki, K. et al. (2006). The Rho-mDia1 pathway regulates cell polarity and focal adhesion turnover in migrating cells through mobilizing Apc and c-Src. *Mol. Cell. Biol.* **26**, 6844-6858.

Yamazaki, D., Oikawa, T. and Takenawa, T. (2006). Rac-WAVE-mediated actin reorganization is required for organization and maintenance of cell-cell adhesion. *J. Cell Sci.* **120**, 86-100.

Zhang, J., Betson, M., Erasmus, J., Zeikos, K., Bailly, M., Cramer, L. P. and Braga, V. M. (2005). Actin at cell-cell junctions is composed of two dynamic and functional populations. *J. Cell Sci.* **118**, 5549-5562.